

43  
N91-19156-70  
30 10  
1  
ND315753  
CR 303094

## AEOLIAN REMOVAL OF DUST TYPES FROM PHOTOVOLTAIC SURFACES ON MARS

James R. Gaier and Marla E. Perez-Davis  
NASA Lewis Research Center  
Cleveland, Ohio 44135

Mark Marabito  
Cleveland State University  
Cleveland, Ohio 44115

ABSTRACT

Dust elevated in local or global dust storms on the Martian surface could settle on photovoltaic (PV) surfaces and seriously hamper their performance. Using a recently developed technique to apply a uniform dust layer, PV surface materials were subjected to simulated Martian winds in an attempt to determine whether natural aeolian processes on Mars would sweep off the settled dust. Three different types of dust were used; an optical polishing powder, basaltic "trap rock", and iron (III) oxide crystals. The effects of wind velocity, angle of attack, height above the Martian surface, and surface coating material were investigated. It was found that arrays mounted with an angle of attack approaching 45° show the most efficient clearing. Although the angular dependence is not sharp, horizontally mounted arrays required significantly higher wind velocities to clear off the dust. From this test it appears that the arrays may be erected quite near the ground, but previous studies have suggested that saltation effects can be expected to cause such arrays to be covered by soil if they are set up less than about a meter from the ground. Particle size effects appear to dominate over surface chemistry in these experiments, but additional tests are required to confirm this. Providing that the surface chemistry of Martian dusts is not drastically different from simulated dust and that gravity differences have only minor effects, the materials used for protective coatings for photovoltaic arrays may be optimized for other considerations such as transparency, and chemical or abrasion resistance. The static threshold velocity is low enough that there are regions on Mars which experience winds strong enough to clear off a photovoltaic array if it is properly oriented. Turbulence fences proved to be an ineffective strategy to keep dust cleared from the photovoltaic surfaces.

INTRODUCTION

In the past few years there has been a growing consensus that the United States will, perhaps in the next 30 years, send a manned spacecraft to land on the surface of Mars. Because of the length of the journey, astronauts will probably stay on the surface for an extended period of time, perhaps several weeks. During their stay there will be power requirements which will exceed those of present spacecraft (ref. 1), and an important component of that power will no doubt be supplied by photovoltaic arrays.

Photovoltaic arrays will be subjected to an environment unlike those in which they have heretofore been used. The atmosphere of Mars consists of CO<sub>2</sub> (95.3 percent), N<sub>2</sub> (2.7 percent), Ar (1.6 percent), O<sub>2</sub> (0.13 percent), CO

(0.07 percent), H<sub>2</sub>O (0.03 percent), and ppm or less of O<sub>3</sub>, Ne, Kr, and Xe (ref. 2). Natural environmental conditions on Mars such as high velocity winds, dust, ultraviolet radiation, rapid temperature changes, soil composition, and atmospheric condensates (H<sub>2</sub>O and CO<sub>2</sub>) may pose a threat to photovoltaic arrays. Results of the soil analysis experiments on board the Viking landers suggest the presence of highly oxidizing species in the soil (ref. 3). Although 99.9 percent of the wind measurements from the Viking landers showed velocities of 20 m/s or less (ref. 4), dust storms were observed to move at higher velocities (up to 32 m/s) (ref. 5), and aeolian features (sand dunes, etc.) suggest that on occasion there are very high winds (>100 m/s) (ref. 6), albeit at low pressure (5 to 8 torr). The surface temperatures range from 135 to 300 K (ref. 7), and daily temperature swings ranging from 20 to 50 K are not uncommon (ref. 8).

One of the possible threats comes from local and/or global dust storms which engulf the planet nearly annually. Infrared spectra from the Mariner 9 spacecraft suggested that the dust is a mixture of many minerals (granite, basalt, basaltic glass, obsidian, quartz, andesite or montmorillonite), and that the average particle size in the atmosphere is about 2  $\mu$ m (ref. 9). A significant amount of dust may be deposited on the array surface during a dust storm (ref. 10) which could occlude the light and significantly degrade the performance of the array. It is not known at this point how serious a problem dust accumulation might be or whether the tenuous but high velocity winds would blow the dust off of the array. Perhaps the photovoltaic array can be designed so as to maximize the ability of the array to be self-clearing.

The purpose of this study is to determine whether dust will be removed from photovoltaic arrays by natural aeolian processes, and how the composition of the dust, the shape and the orientation of the array can affect this process.

The authors would like to thank R. Leach of Arizona State University and the support staff at NASA Ames Research Center for their thought-provoking discussions and essential assistance with the MARSWIT facility. We would like to acknowledge the contributions of S.K. Rutledge of NASA Lewis Research Center, J. Mihelcic of Cleveland State University, and M. Kussmaul of Sverdrup Technology, Inc. for their assistance in preparing the optical coatings. J. Tillman and R. Greeley provided us with helpful discussions and expertise on the Martian environment.

## METHODS AND MATERIALS

There are a variety of variables which could effect dust removal from a photovoltaic surface on Mars. In these tests we evaluated the effects of photovoltaic cell surface, angle of attack, wind velocity, height from the planetary surface, and turbulence. In addition, we used three different dust types to determine the effects of particle size and composition.

Glass coverslips 2.54 cm<sup>2</sup>, and 0.13 mm thick were used for the sample substrates. These were left bare or ion beam sputter deposited with a coating of SiO<sub>2</sub>, polytetrafluoroethane (PTFE), 50 percent mixture of SiO<sub>2</sub> and PTFE,

indium tin oxide (ITO), or diamond-like carbon (DLC). Table I summarizes the coatings. These coatings were chosen because they are candidate materials for protective coatings for photovoltaic arrays. The substrates were thin, both to minimize turbulence and for low mass, to improve the accuracy of weight determinations of the dusted substrates.

The samples were mounted in specially designed sample holders by means of foil tabs which stretched across two corners, and held down by a foil tab attached to a removable pin (see fig. 1). Samples were held at a tilt angle of 0°, 22.5°, 45°, 67.5°, or 90° from horizontal. The sample holders could also be held horizontally for dust deposition and optical transmittance measurements.

Initially, the sample holders were tilted so that the samples were held horizontally, and then subjected to a dusting which simulates dust accumulation in the aftermath of a dust storm. The method of dusting and the resulting dust distribution are discussed in detail elsewhere (ref. 11).

The composition of the Martian dust is not well understood. The elemental composition was determined by the Viking landers (ref. 12), and based on optical properties developed from terrestrial minerals, analogs have been proposed (ref. 9). The Viking biology experiments, however, dramatically showed that the chemistry of the dust is unique to Mars. Three different types of dust were chosen for preliminary experiments to determine how large a role the chemical composition might play in dust clearing from power surfaces.

The first dust used in these experiments was 1800 grit optical grinding powder from American Optical Company. It is principally an aluminum oxide powder which is not greatly affected by moisture in the air. This powder showed the least tendency of the three to agglomerate, and so gave us the cleanest distribution of particles on the surfaces.

The second dust was a basalt known as trap rock which is thought to be similar in properties to the Martian dust. This material, while our best approximation of Martian dust, did show some agglomeration. The fact that the dust is a grey-green color also indicates differences from the orange Martian dust.

The third dust was iron (III) oxide. Higher oxides of iron have been invoked to explain the Viking biology experiments, and are thought to be present in Martian dust. The particle size of this material was an order of magnitude smaller than that of the other two materials.

The elemental composition and particle size of the three dusts used in this experiment are compared to that of the Martian dust in table II. However, it should be noted that the purpose of this experiment was not to try to accurately simulate the Martian soil, but to try to determine how sensitive dust clearing is to composition. Also, although the values for dust clearing wind velocities on Mars may differ from those in these simulation experiments, the order of magnitude and the trends in angle and height from the surface are expected to be similar.

Because of size limitations imposed by the dusting apparatus, no more than four sample holders could be dusted at once. The amount of dust which accumulated on the samples was difficult to control, being critically dependent upon the amount of dust in the chamber, the height to which the dust is elevated, the pressure, and the time allowed for larger particles to settle out. Thirteen dusting runs were required for this study, and the resulting samples had ratios of transmittance of the dusted samples ( $T_d$ ) to transmittance of the pristine samples ( $T_0$ ) which were as low as 0.18 and others as high as 0.89. The spatial uniformity of each dusting operation was much better. The  $T_d/T_0$  for each sample is shown in figure 2.

The winds on Mars were simulated using the Martian Surface Wind Tunnel (MARSWIT) at NASA Ames Research Center. The MARSWIT is a low pressure (down to a few hundred Pa) wind tunnel 14 m in length with a 1 by 1.1 by 1.1 m test section located 5 m from the tunnel entrance. This flow-through wind tunnel is located within a 4000 m<sup>3</sup> vacuum chamber. The windtunnel injected either CO<sub>2</sub> (for the aluminum oxide samples) or air (for the basalt and iron oxide samples) to create the windflow. Its characteristics are described in detail elsewhere (ref. 13). The samples were placed in the MARSWIT and tested under the wind conditions listed in table III.

The samples were weighed before dusting, after dusting, and after MARSWIT exposure. However, the weight of the dust added to the optical surfaces was below the sensitivity of the balance used (0.1 mg).

Optical transmittance measurements were made by sliding the transmittance measurement device (TMD) over the sample. In the TMD a white light source is suspended above the sample, and the sensing head of a Coherent Model 212 Power Meter is beneath the sample. Specular transmittance measurements were made before and after the samples were dusted ( $T_0$  and  $T_d$ , respectively), and after the dusted samples were subjected to winds in the MARSWIT ( $T_f$ ).

The amount of dust which was cleared from the samples was evaluated using a dust clearing parameter, which was defined as the ratio of the transmittance change on wind exposure of the dusted samples ( $T_f - T_d$ ) to that of the transmittance change upon dusting ( $T_0 - T_d$ ). This function is a transmittance recovery fraction and is constrained to vary from zero to one. There is, unfortunately, a dependence of the value of  $T_d$  used in different sample dustings on this parameter.

The final transmittance ( $T_f$ ) is a function of wind velocity, angle to the wind, surface chemistry, particle size, and time. It may also be a function of the amount of dust initially deposited assuming that the degradation of  $T_f$  from  $T_0$  arises solely from particles remaining on the surface. Typically, the particles are sufficiently small that surface adhesion is stronger than the forces that can be exerted by the dynamic pressure of the wind. The number of particles at the surface interface will increase as the total number of particles dusted on the sample increases (i.e., as  $T_d$  decreases) up until a monolayer is built up. Beyond that there is only particle-particle cohesion. Thus,  $T_f$  will be a function of  $T_d$  until the monolayer is established, and beyond that it will not. If  $T_f$  is a function of  $T_d$  then, for dusting runs of low  $T_d$ , the dust clearing parameter would take a higher value for the same

dust clearance effectiveness. For dusting runs of high  $T_d$ , the dust clearing parameter should be independent of  $T_d$ .

Two different heights from the floor of the wind tunnel were used for dust clearing tests using the aluminum oxide dust. Samples were placed at about 2.5 cm, which should be within the floor's boundary layer, and at about 50 cm, which should be well above it.

A turbulence fence was constructed to increase the wind turbulence at the sample. It was thought that the turbulent flow might be effective at clearing the dust at wind speeds lower than those in the free stream. It was constructed with a vertical array of eight 3.2 mm diameter horizontal rods spaced every 9.5 mm.

## RESULTS AND DISCUSSION

The two most important variables to dust clearing efficiency were found to be the angle of attack and the velocity of the wind. Accordingly, they will be discussed first, and turbulence and coating material will be discussed as small perturbations on the effects.

Higher wind velocities are expected to clear photovoltaic surfaces more effectively. It might also be suspected that there will be a threshold value for the wind velocity below which there will be no clearing, and above which, given sufficient time there will be significant, perhaps even total clearing. The static threshold velocity is that velocity at which dust particles leave the surface without impact from upwind particles. There are several factors which will affect the static threshold velocity including particle size, particle shape, and surface chemistry. In these experiments the particle size was chosen to match that which it is believed to become suspended during a global dust storm, but which would settle out under calmer conditions. Particles less than about 1  $\mu\text{m}$  in size will stay suspended for very long periods of time, and those larger than about 50  $\mu\text{m}$  will never be transported far from the site where they first become airborne. The particles used in this experiment mimic the Martian dust size and shape (ref. 11), the surface chemistry of the particles, however, is likely to be quite different from that found on Mars.

Soils on Mars are thought to be basaltic, and rich in iron oxides (ref. 9). Further, the Viking results infer the possibility of peroxide and superoxides which may be generated by the ultra-violet radiation that constantly bombards the surface (ref. 5). Accurate duplication of the exotic Martian surface chemistry is difficult at the present time due to the limited understanding of Martian soil composition. In addition, the presence of much more water vapor in the Earth environment would change the surface chemistry even if we did know how to simulate Martian soil. The optical polishing powder has been shown to dust the samples evenly with little particle aggregation (ref. 11). Thus, this material is a reasonable starting point for these studies, and that trends in angle, height, turbulence, etc. should still be valid. In addition, results of experiments to determine the threshold dust clearing values for the basalt and iron oxide, which have different surface chemistries, were compared to evaluate its effect.

Figure 3 shows the dust clearing as a function of angle for various velocities of simulated Martian wind using the aluminum oxide dust. The amount that some of the data points lie below zero give some indication of the experimental error. There is a clear indication from figure 3 that the optimum value was near  $45^\circ$ . Samples with an attack angle of zero showed virtually no dust clearing at velocities below about 100 m/s, while those at  $45^\circ$  cleared to about 92 percent of their original transmittance value at wind velocities as low as 35 m/s. Samples held at angles of  $22.5^\circ$  and  $67.5^\circ$  cleared slightly less efficiently than those at  $45^\circ$ . Samples held at  $90^\circ$  showed still less clearing, but more than those held at  $0^\circ$ . This trend was found with velocities varying from 30 to 85 m/s. In the test with a higher velocity (124 m/s) all of the samples were cleared comparably. In the test with a lower velocity (10 m/s) none of the samples cleared appreciably. Note that the time exposed to the wind was not the same in all cases (see table I), but the angular dependence of dust clearing is not expected to be time dependent.

In one series of samples in the 85 m/s wind test, vertical ( $90^\circ$ ) sample holders were angled at  $0^\circ$ ,  $30^\circ$ ,  $60^\circ$ , and  $90^\circ$  from the wind around a vertical axis. This should be an equivalent configuration to having samples on  $0^\circ$ ,  $30^\circ$ ,  $60^\circ$ , and  $90^\circ$  tilts, provided gravity does not play a significant role. The angular dependence was indeed consistent with the other experiments (see fig. 3).

The threshold clearing velocity predicted by Iverson and White is considerably below the measured values (ref. 14). Using the  $0^\circ$  data we find a threshold velocity of somewhat less than 85 m/s, about an order of magnitude higher than predicted. The experimental conditions, however, were not the same as the theoretical assumptions. Iverson and White assumed a layer of spherical particles laying on a bed of similar particles. In the experiment, there was less than a monolayer of non-spherical particles on various substrates. Intuitively, however, one might expect the threshold velocity to be smaller in the experiment because of the smooth substrate.

Given the angular dependence of the dust clearing, one might suspect that the mechanism of detachment would involve the rolling or sliding of dust particles. For the most part, however, this did not appear to be the case. Photomicrographs of the dust layer remaining on dusted glass surfaces subjected to 35 m/s winds at different attack angles showed no directionality to the dust removal. Only on the samples with an attack angle of  $22.5^\circ$  could it be discerned from the photographs the direction of the wind arrival. This was further confirmed by the photograph of a half-round sample subjected to the same conditions. Only as the attack angle became very low was there appreciable streaking. Thus, turbulence at the surface must act to aerodynamically lift the particles out in a direction which is approximately normal to the surface. This view is supported by classical models of Bagnold (ref. 15) in which aerodynamic lift plays a key role in particle motion from a surface at the threshold velocity.

Given the cautions above, the static threshold velocity to remove dust particles from the surface was determined. The data taken at  $45^\circ$  is of most interest, because that will give us the minimum static threshold value. In figure 4 it can be seen that the minimum threshold value for the optical

polishing grit was between 30 and 35 m/s. Although this is higher than the average daily maximum wind speed at the Viking landing sites of about 9 m/s (ref. 16), it is not uncommon on some parts of the Martian surface (ref. 5).

The importance of turbulence in the clearing of dust from surfaces was studied from two different sources: boundary-layer turbulence, and artificially induced turbulence. Turbulence will result in a lower mean velocity (and so a lower mean dynamic pressure to move the particles) but it may result in higher local velocities.

Identical samples were run at about 3 cm and about 50 cm from the floor of the MARSWIT. Figure 5 shows the approximate height of the boundary layer (where the velocity becomes the free-stream velocity) at several different velocities and the height of the samples. It can be seen that the lower samples were within the boundary layer, and the upper ones were not. As can be noted from figure 6, however, there was no appreciable differences between these two heights. In one experiment, in a 55 m/s wind, a sample holder was placed on end so as to fix the samples nearer to the floor. The holder was placed at a 45° angle to maximize the dust clearing. Figure 7 shows that in this extreme case there may have been small boundary layer effects observed, with the lower samples showing slightly less clearing.

Turbulence was also induced by placing a "fence" of cylindrical rods in front of the samples at a wind speed near the threshold. The hope was that the turbulence fence would lower the threshold wind speed, but the fence was found to actually hinder the clearing slightly (see fig. 8).

A wide variety of photovoltaic cell coatings was tested to determine which coatings would be most effective in shedding the dust. Because of the probable differences in surface chemistry between the test material and actual Martian soils this is risky, but perhaps some general surface principles can be determined. Even though there was a wide variety of materials both conducting and insulating, hard and soft, and high and low coefficients of friction, there were only slight differences among the ability of the coatings to shed the dust. For each angle of attack (0°, 22.5°, 45°, 67.5°, and 90°) and for wind velocities of 55, 85, and 124 m/s, each coating was ranked on the basis of dust clearing parameter from highest (1) to lowest (3 or 6, depending on the number of samples). The average ranking over all of the angles at a given wind speed for each of the coatings is shown in table IV. The last column in table IV shows the average ranking for each coating over all of the angles and all of the wind speeds. Although the error is probably large, there may be some validity to the rankings. Glass and SiO<sub>2</sub> have nearly equal scores, as do PTFE and PTFE/SiO<sub>2</sub>. ITO was the easiest to clear, and DLC the hardest. Surface adhesion tests are planned to test the validity of the ranking.

The dust clearing using basalt instead of aluminum oxide produced similar results, as illustrated in figure 9. The threshold velocity at 45° appears to be between 30 and 40 m/s, within the same range as the aluminum oxide. From this test it appears that surface chemistry (within limits) does not play a large role in determining the dust clearing threshold velocity. Given the uncertainties in knowledge of Martian dust, this is fortunate.

However, when iron oxide dust was used the threshold velocity was much higher, between 85 and 95 m/s, as shown in figure 10. The surface chemistry of iron oxide differs considerably from either of the other two materials, and that could certainly affect the results. However, a more important effect may well be the particle size. The mean particle size of the iron oxide is an order of magnitude smaller than that of the other two materials, and so one would expect the threshold velocity to be between two and three times higher based on particle size effects alone (ref. 17). Further studies are required to separate particle size from surface chemistry effects in any definitive way.

The angular dependences of the threshold velocity for the basalt and the iron oxide raise some interesting questions. In the case of basalt in 30 m/s winds it can be seen in figure 9 that there is more efficient clearing at 22.5° than at 45°. Streaks which indicate the wind direction are also visible in the 22.5° case. It appears that at low angles the particles begin to roll off the surface. The threshold velocity for this is evidently somewhat lower than for the aerodynamic lift removal that is dominant at higher angles. It appears then, that the aerodynamic removal is more efficient, but requires a somewhat higher velocity.

Figure 10 reveals that iron oxide was most efficiently removed at 22.5° at wind velocities even as high as 95 m/s. This could have two possible explanations. The first is that this velocity is not high enough for the aerodynamic lift mechanism to begin to dominate, or in other words, the aerodynamic threshold velocity still had not been reached. The second explanation is that particle size effects cause the rolling dust clearing to dominate at all velocities, that is, that even at much higher velocities the 22.5° samples would have cleared more efficiently.

## CONCLUSIONS

Even in this first preliminary study principles have been found which can help to guide the design of photovoltaic arrays bound for the Martian surface. Most importantly, if an array is to be self-cleaning it should be tilted at an angle approaching 45°. Although there is wide latitude with this requirement, it seems most important that the arrays are not erected horizontally. Although the angular dependence is not sharp, horizontally mounted arrays required significantly higher wind velocities to clear off the dust. From the perspective of dust clearing it appears that the arrays may be erected quite near the ground, but saltation can be expected to cover the arrays if they are set up less than about a meter from the ground (ref. 18). Providing that the surface chemistry of Martian dusts is comparable to the simulated test dusts, the materials used for protective coating may be optimized for other considerations such as transparency, and chemical or abrasion resistance. Given the same assumption, there are regions on Mars which experience winds strong enough to clear off a photovoltaic array which is properly oriented, though there are other regions where some other clearing technique will have to be employed. Turbulence fences proved to be an ineffective strategy to keep dust cleared from the photovoltaic surfaces.



There seem to be two dust removal mechanisms at work. At low angles (22.5° and less) the dust particles are rolled off of the surface, and at high angles (45° and higher) the particles are aerodynamically lifted from the surface. The threshold value for the rolling mechanism appears to be lower, but the aerodynamic lift mechanism appears to be more effective.

#### REFERENCES

1. Giudici, R.J.: Electrical Power Systems for Mars. The Case for Mars: Proceedings of a Conference, American Astronautical Society, 1983, pp. 873-887.
2. Owen, T.K.; Biemann, K.; Rushneck, D.R.; Biller, J.E.; Howarth, D.W.; and Lefleur, A.L.: The Composition of the Atmosphere at the Surface of Mars. *J. Geophys. Res.*, vol. 82, Sept. 30, 1977, pp. 4635-4639.
3. Klein, H.P.: Viking Biological Experiments on Mars. *Icarus*, vol. 34, no. 3, 1978, pp. 666-674.
4. Kaplan, D.: Environment of Mars. NASA TM-100470, 1988.
5. Peterfreund, A.R.; and Kieffer, H.H.: Thermal Infrared Properties of the Martian Atmosphere. III - Local Dust Clouds. *J. Geophys. Res.*, vol. 84, June 10, 1979, pp. 2853-2863.
6. Pollack, J.B.; Colburn, D.S.; Flasar, F.M.; Hahn, R.; Carlston, C.E.; and Pidek, D.: Properties and Effects of Dust Particles Suspended in the Martian Atmosphere. *J. Geophys. Res.*, vol. 84, June 10, 1979, pp. 2929-2945.
7. Kieffer, H.H.; Martin, T.Z.; Peterfreund, A.R.; Jakosky, B.M.; Miner, E.D.; and Palluconi, F.D.: Thermal and Albedo Mapping of Mars During the Viking Primary Mission. *J. Geophys. Res.*, vol. 82, Sept. 30, 1977, pp. 4249-4291.
8. Tillman, J.E.: Martian Meteorology and Dust Storms from Viking Observations. The Case for Mars, II: Proceedings of the Conference, American Astronautical Society, 1985, pp. 333-342.
9. Toon, O.B.; Pollack, J.B.; and Sagan, C.: Physical Properties of the Particles Composing the Martian Dust Storm of 1971-1972. *Icarus*, vol. 30, Apr. 1977, pp. 663-696.
10. Arvidson, R.E.; Guinness, E.A.; Moore, H.J.; Tillman, J.; and Wall, S.D.: Three Mars Years, Viking Lander 1 Imaging Observations. *Science*, vol. 222, Nov. 4, 1983, pp. 463-468.
11. Perez-Davis, M.E.; Gaier, J.R.; Kress, R.; and Grimalda, J.: Simulation of Martian Dust Accumulation on Surfaces. Sixteenth AIAA-NASA/ASTM/IEA Space Simulation Conference, NASA CP- , 1989. (Paper of this compilation.)

12. Toulmin III, P.; Baird, A.K.; Clark, B.C., Keil, K.; Rose, Jr. H.J.; Christian, R.P.; Evans, P.H.; and Kelliher, W.C.: Geochemical and Mineralogical Interpretation of the Viking Inorganic Chemical Results - for Martian Surface Materials. *J. Geophys. Res.*, vol. 82, Sept. 30, 1977, pp. 4625-4634.
13. Greeley, R.; White, B.R.; Pollack, J.B.; Iversen, J.D.; and Leach, R.N.: Dust Storms on Mars: Considerations and Simulations. NASA TM-78423, 1977.
14. Iversen, J.D.; and White, B.R.: Saltation Threshold on Earth, Mars, and Venus. *Sedimentology*, vol. 29, no. 1, 1982, pp. 111-119.
15. Bagnold, R.A.: The Flow of Cohesionless Grains in Fluids. *Philos. Trans. R. Soc., Ser. A*, vol. 249, 1956, pp. 239-297.
16. Pollack, J.B.; Leovy, C.B.; Mintz, Y.H.; and Van Camp, W.: Winds on Mars During the Viking Season - Predictions Based on a General Circulation Model with Topography. *Geophys. Res. Lett.*, vol. 3, Aug. 1976, pp. 479-482.
17. Iversen, J.D.; Greeley, R.; and Pollack, J.B.: Windblown Dust on Earth, Mars, and Venus. *J. Atmos. Sci.*, vol. 33, Dec. 1976, pp. 2425-2429.
18. Greeley, R.; and Iversen, J.D.: *Wind as a Geological Process: On Earth, Mars, Venus, and Titan.* Cambridge University Press, 1985.

TABLE I. - PHOTOVOLTAIC ARRAY COATINGS TESTED

Coating	Thickness	Deposition	Substrate
None	-----	-----	Glass
SiO <sub>2</sub>	650Å	Ion beam	Glass
PTFE	≈1000Å	Ion beam	Glass
50 percent/ SiO <sub>2</sub>	≈1000Å	Ion beam	Glass
ITO	≈1000Å	Ion beam	Glass
DLC	≈1000Å	Ion beam	Glass

TABLE II. - COMPOSITION OF DUSTS

	Percent by weight			
	Viking	Opt Grt	Basalt	Fe <sub>2</sub> O <sub>3</sub>
SiO <sub>2</sub>	44.7	6.6	46.6	0
Fe <sub>2</sub> O <sub>3</sub>	18.1	0.6	13.0	100
MgO	8.3	0.0	6.1	0
Al <sub>2</sub> O <sub>3</sub>	5.7	89.0	16.6	0
CaO	5.6	0.0	11.1	0
TiO <sub>2</sub>	0.9	3.0	2.0	0
Cr <sub>2</sub> O <sub>3</sub>	0.0	0.6	0.0	0
Na <sub>2</sub> O	?	0.0	2.3	0
K <sub>2</sub> O	0.0	0.0	1.1	0
MnO	0.0	0.0	0.3	0
CO <sub>2</sub>	?	0.0	0.1	0
P <sub>2</sub> O <sub>5</sub>	0.0	0.0	0.1	0
Size, μm		7 to 25	5 to 20	0.5 to 2.5

TABLE III. - WIND CONDITIONS WITHIN THE MARSWIT

Velocity, m/s	Stat Pres, Pa	Dyn Pres, Pa	Temp, K	Time, sec	Dust
10	1000	1.2	290	600	Al <sub>2</sub> O <sub>3</sub>
23	1000	6.3	290	600	Al <sub>2</sub> O <sub>3</sub>
30	1000	10.7	290	600	Al <sub>2</sub> O <sub>3</sub>
30	1000	10.9	285	300	Fe <sub>2</sub> O <sub>3</sub>
31	1000	11.4	290	900	Al <sub>2</sub> O <sub>3</sub>
31	850	9.9	285	600	Basalt
35	1000	14.5	290	300	Al <sub>2</sub> O <sub>3</sub>
42	950	20	285	600	Basalt
50	1000	30	285	90	Fe <sub>2</sub> O <sub>3</sub>
55	1000	36	290	120	Al <sub>2</sub> O <sub>3</sub>
60	1000	43	285	600	Fe <sub>2</sub> O <sub>3</sub>
85	1000	86	290	30	Al <sub>2</sub> O <sub>3</sub>
85	900	78	285	600	Fe <sub>2</sub> O <sub>3</sub>
95	1200	131	285	600	Fe <sub>2</sub> O <sub>3</sub>
124	1000	182	290	45	Al <sub>2</sub> O <sub>3</sub>

TABLE IV. - RELATIVE EASE OF DUST CLEARANCE FROM  
PHOTOVOLTAIC COATINGS

Coating	55 m/s	85 m/s	124 m/s	Overall
ITO	1.0	1.6	2.5	1.9
PTFE/SiO <sub>2</sub>	1.0	1.8	3.0	2.2
PTFE	2.0	2.3	2.3	2.3
SiO <sub>2</sub>	3.0	1.9	3.6	2.8
Glass	2.0	2.4	3.8	2.9
DLC	3.0	2.1	4.3	3.2

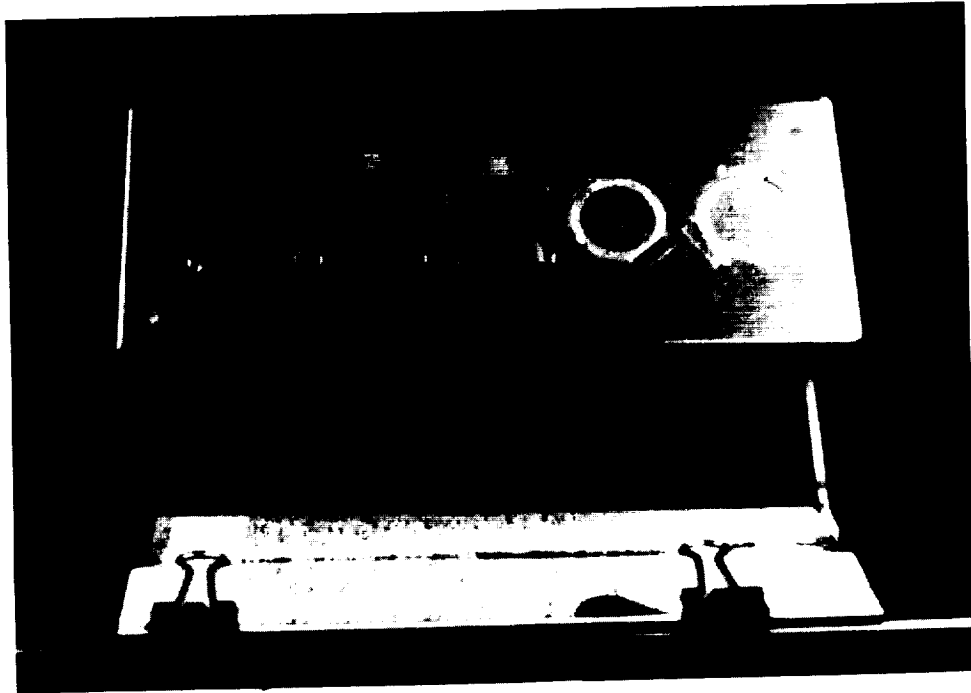


Figure 1. Sample Holder Designed to Test Aeolian Dust Removal from Photovoltaic Surfaces

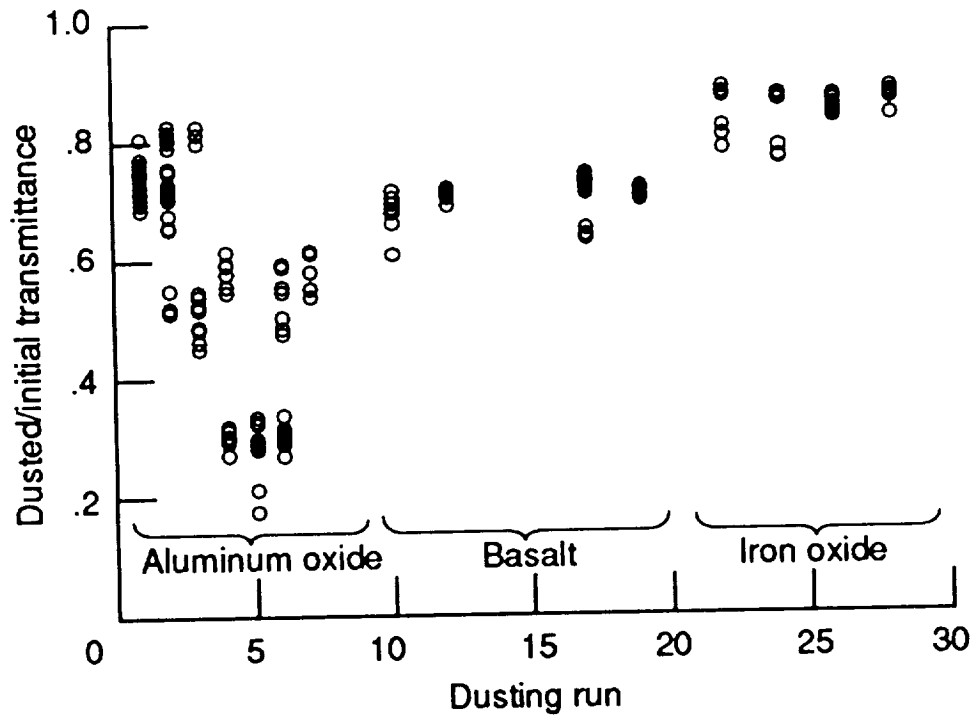


Figure 2. Uniformity of Dust Deposition

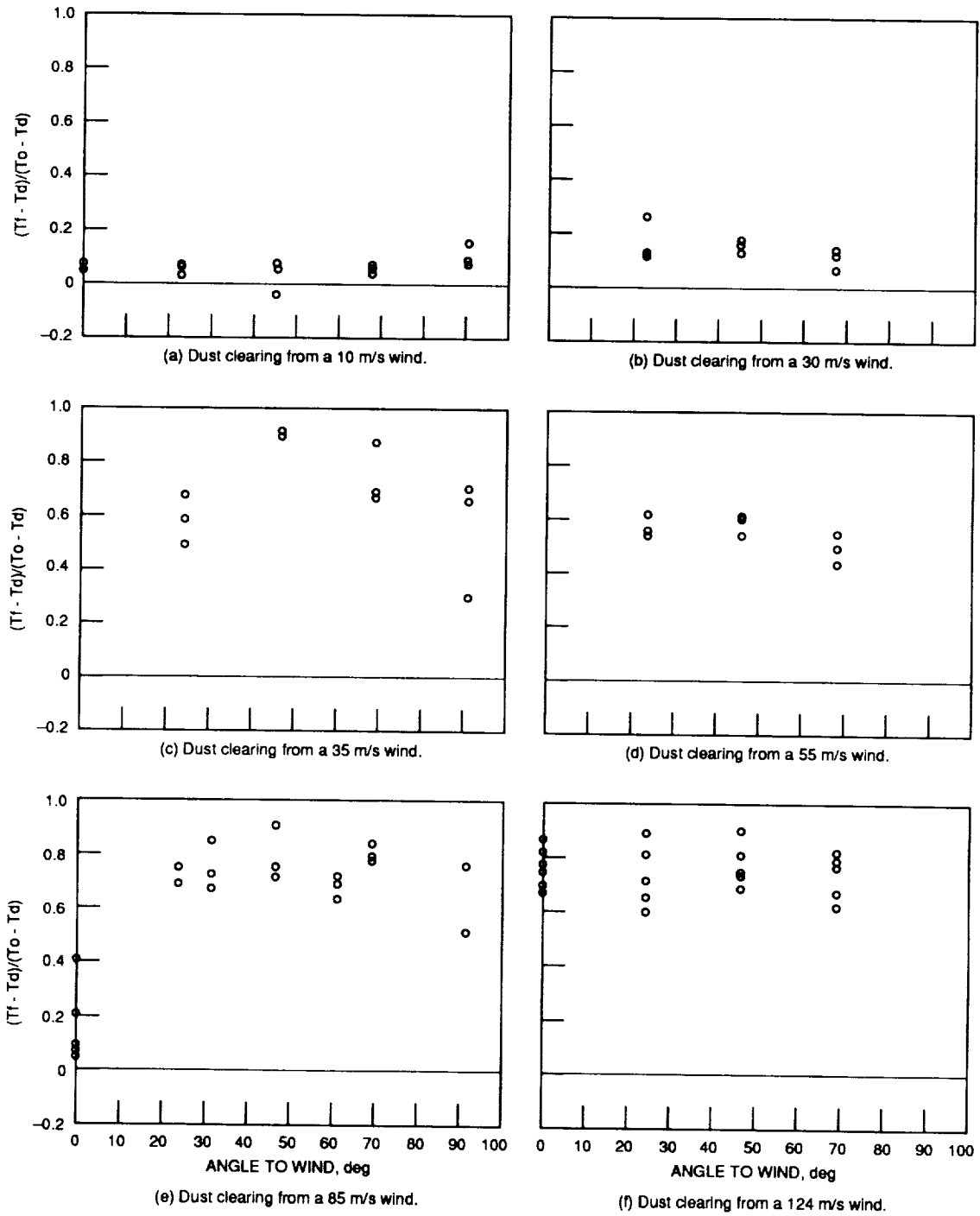


Figure 3. Dust Clearing as a Function of Angle for Several Different Martian Wind Speeds



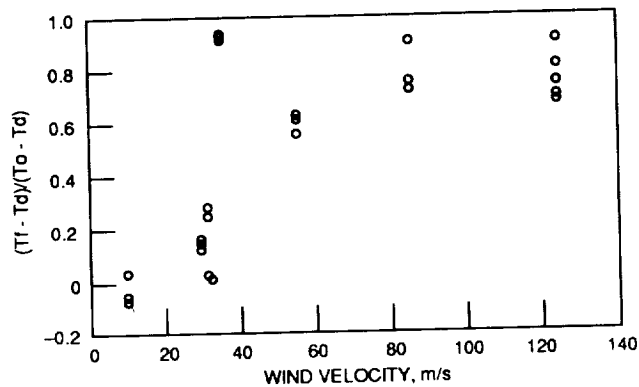


Figure 4. Dust Clearing from a Smooth 45° Angle Surface

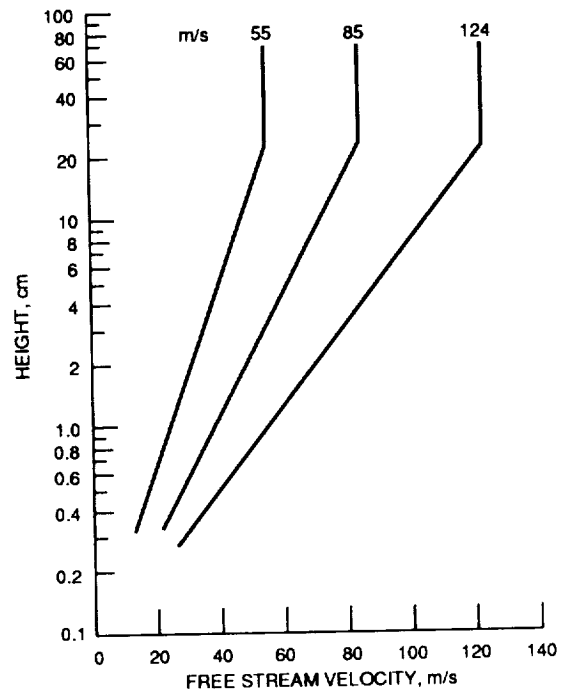


Figure 5. Nominal Boundary Layer Profiles

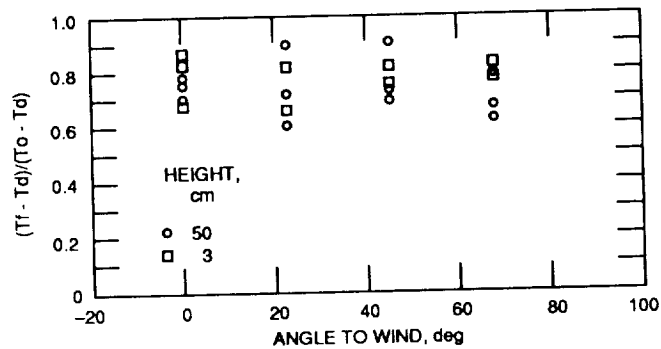


Figure 6. Dust Clearing at Different Heights from Wind Tunnel Floor

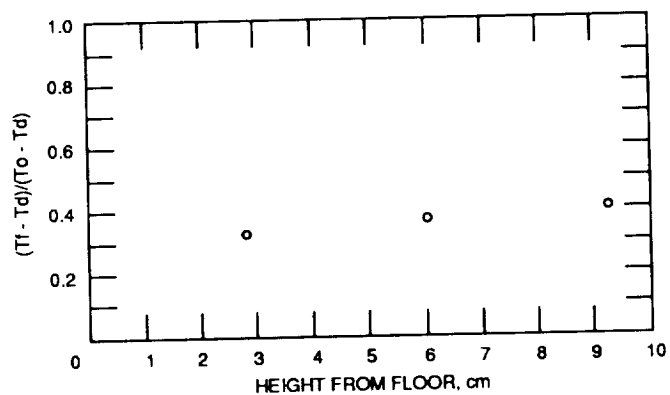


Figure 7. Dust Clearing in Boundary Layer at 55 m/s

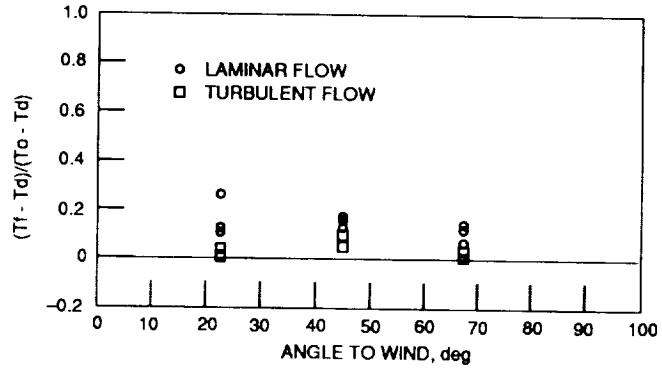


Figure 8. Dust Clearing from a 30 m/s Wind

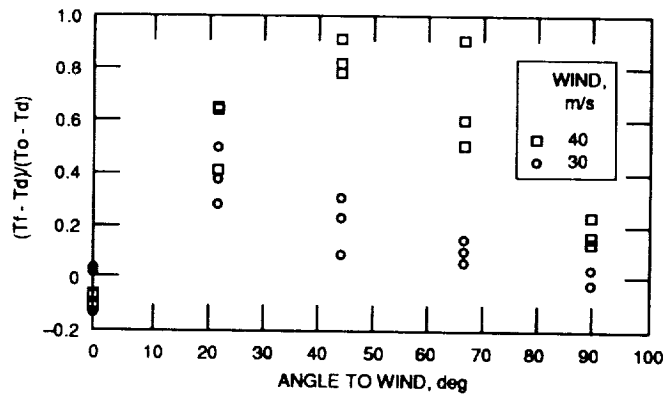


Figure 9. Trap Rock Dust Clearing

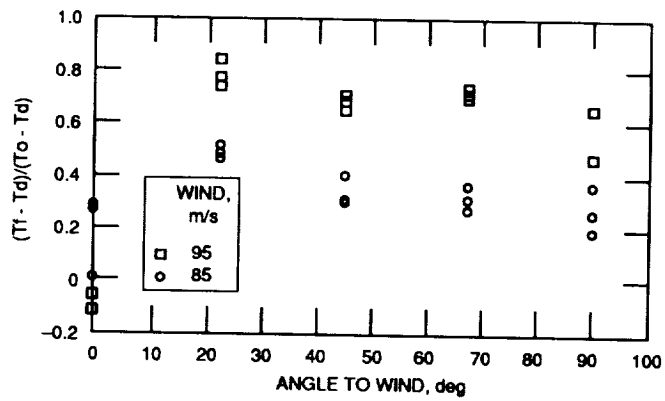


Figure 10. Iron Oxide Dust Clearing